You Can Have Better Graph Neural Networks by Not Training Weights at All: Finding Untrained GNNs Tickets

Anonymous Author(s)
Anonymous Affiliation
Anonymous Email

Abstract

Recent works have impressively demonstrated that there exists a subnetwork in randomly initialized convolutional neural networks (CNNs) that can match the performance of the fully trained dense networks at initialization, without any optimization of the weights of the network (i.e., untrained networks). However, the presence of such untrained subnetworks in graph neural networks (GNNs) still remains mysterious. In this paper we carry out the first-of-its-kind exploration of discovering matching untrained GNNs. With sparsity as the core tool, we can find *untrained sparse subnetworks* at the initialization, that can match the performance of *fully trained dense* GNNs. Besides this already encouraging finding of comparable performance, we show that the found untrained subnetworks can substantially mitigate the GNN over-smoothing problem, hence becoming a powerful tool to enable deeper GNNs without bells and whistles. We also observe that such sparse untrained subnetworks have appealing performance in out-of-distribution detection and robustness of input perturbations. We evaluate our method across widely-used GNN architectures on various popular datasets including the Open Graph Benchmark (OGB). Our source codes are submitted in the Supplementary.

1 Introduction

Graph Neural Networks (GNNs) [1, 2] have shown the power to learn representations from graph-structured data. Over the past decade, GNNs and their variants such as Graph Convolutional Networks (GCN) [3], Graph Isomorphism Networks (GIN) [4], Graph Attention Networks (GAT) [5] have been successfully applied to a wide range of scenarios, e.g., social analysis [6, 7], protein feature learning [8], traffic prediction [9], and recommendation systems [10]. In parallel, works on untrained networks [11, 12] surprisingly discover the presence of untrained subnetworks in CNNs that can already match the accuracy of their fully trained dense CNNs with their initial weights, without any weight update. In this paper, we attempt to explore discovering untrained sparse networks in GNNs by asking the following question:

Is it possible to find a well-performing graph neural (sub-) network without any training of the model weights?

Positive answers to this question will have significant impacts on the research field of GNNs. ① If the answer is yes, it will shed light on a new direction of obtaining performant GNNs, e.g., traditional training might not be indispensable towards performant GNNs. ② The existence of such performant subnetworks will extend the recently proposed untrained subnetwork techniques [11, 12] in GNNs. Prior works [11–13] successfully find that randomly weighted full networks contain untrained subnetworks which perform well without ever modifying the weights, in convolutional neural networks (CNNs). However, the similar study has never been discussed for GNNs. While CNNs reasonably contain well-performing untrained subnetworks due to heavy over-parameterization, GNN models are usually much more compact, and it is unclear whether a performant subnetwork "should" still exist in GNNs.

Submitted to the First Learning on Graphs Conference (LoG 2022). Do not distribute.

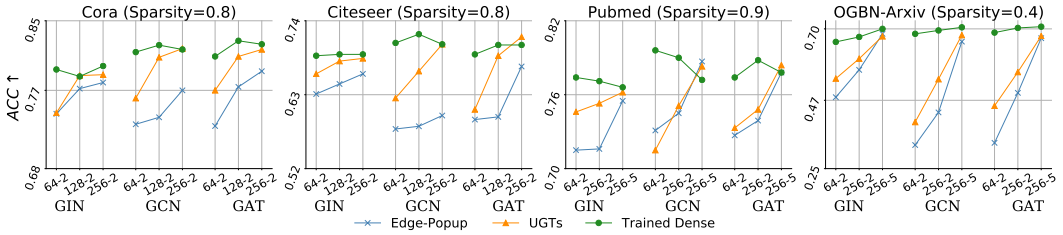

Figure 1: Performance of untrained graph subnetworks (UGTs (ours) and Edge-Popup [12]) and the corresponding trained dense GNNs. We demonstrate that as the model size increases, UGTs is able to find an untrained subnetwork with its random initializations, that can match the performance of the corresponding fully-trained dense GNNs. The x-axis denotes the corresponding model size for each point, e.g. "64-2" represents a model with 2 layers and width 64.

Furthermore, we investigate the connection between untrained sparse networks and widely-known barriers in deep GNNs, such as over-smoothing. For instance, as analyzed in [14], by naively stacking many layers and adding non-linearity, the output features are prone to collapsing and becoming indistinguishable. Such undesirable properties significantly limit the power of deeper/wider GNNs, hindering the potential application of GNNs on large-scale graph datasets such as the latest Open Graph Benchmark (OGB) [15]. It is interesting to see what would happen for untrained graph neural networks. Note that the goal of sparsity in our paper is **not for efficiency**, but to obtain nontrivial predictive performance without training (a.k.a., "masking is training" [11]). We summarize our contributions as follows:

- We demonstrate for the first time that there exist untrained graph subnetworks with matching performance (referring to as good as the trained full networks), **within randomly initialized dense networks and without any model weight training**. Distinct from the popular lottery ticket hypothesis (LTH) [16, 17], neither the original dense networks nor the identified subnetworks need to be trained.
- We find that the gradual sparsification technique [18, 19] can be a stronger performance booster. Leveraging its global sparse variant [20], we propose our method – UGTs, which discovers matching untrained subnetworks within the dense GNNs at extremely high sparsities. For example, our method discovers untrained matching subnetworks with up to 99% sparsity. We validate it across various GNN architectures (GCN, GIN, GAT) on eight datasets, including the large-scale OGBN-ArXiv and OGBN-Products.
- We empirically show a surprising observation that our method significantly mitigates the over-smoothing problem without any additional tricks and can successfully scale GNNs up with negligible performance loss. Additionally, we show that UGTs also enjoys favorable performance on Out-of-Distribution (OOD) detection and robustness on different types of perturbations.

2 Related Work

Graph Neural Networks. Graph neural networks is a powerful deep learning approach for graph-structured data. Since proposed in [1], many variants of GNNs have been developed, e.g., GAT [5], GCN [3], GIN [4], GraphSage [21], SGC [22], and GAE [23]. More and more recent works point out that deeper GNN architectures potentially provide benefits to practical graph structures, e.g., molecules [8], point clouds [24], and meshes [25], as well as large-scale graph dataset OGB. However, training deep GNNs usually is a well-known challenge due to various difficulties such as gradient vanishing and over-smoothing problems [14, 26]. The existing approaches to address the above-mentioned problem can be categorized into three groups: (1) skip connection, e.g., Jumping connections [27, 28], Residual connections [24], and Initial connections [29]; (2) graph normalization, e.g., PairNorm [26], NodeNorm [30]; (3) random dropping including DropNode [31] and DropEdge [32].

Untrained Subnetworks. Untrained subnetworks refer to the hypothesis that there exists a subnetwork in a randomly intialized neural network that can achieve almost the same accuracy as a fully trained neural network without weight update. [11] and [12] first demonstrate that randomly

initialized CNNs contain subnetworks that achieve impressive performance without updating weights at all. [13] enhanced the performance of untrained subnetworks by iteratively reinitializing the weights that have been pruned. Besides the image classification task, some works also explore the power of untrained subnetworks in other domains, such as multi-tasks learning [33] and adversarial robustness [34].

Instead of proposing well-versed techniques to enable deep GNNs training, we explore the possibility of finding well-performing deeper graph subnetworks at initialization in the hope of avoiding the difficulties of building deep GNNs without model weight training.

3 Untrained GNNs Tickets

3.1 Preliminaries and Setups

Notations. We represent matrices by bold uppercase characters, e.g. $\boldsymbol{X}$, vectors by bold lowercase characters, e.g. $\boldsymbol{x}$, and scalars by normal lowercase characters, e.g. x. We denote the i^{th} row of a matrix $\boldsymbol{A}$ by $\boldsymbol{A}[i,:]$, and the $(i,j)^{th}$ element of matrix $\boldsymbol{A}$ by $\boldsymbol{A}[i,j]$. We consider a graph $\mathcal{G} = \{\mathcal{V}, \mathcal{E}\}$ where $\mathcal{E}$ is a set of edges and $\mathcal{V}$ is a set of nodes. Let $g(\boldsymbol{A}, \boldsymbol{X}; \boldsymbol{\theta})$ be a graph neural network where $\boldsymbol{A} \in \{0,1\}^{|V|\times|V|}$ is adjacency matrix for describing the overall graph topology, and $\boldsymbol{X}$ denotes nodal features . $\boldsymbol{A}[i,j] = 1$ denotes the edge between node v_i and node v_j. Let $f(\boldsymbol{X}; \boldsymbol{\theta})$ be a neural network with the weights $\boldsymbol{\theta}$. $\|\cdot\|_0$ denotes the L_0 norm.

Sparse Neural Networks. Given a dense network $\boldsymbol{\theta_l} \in \mathcal{R}^{d_l}$ with a dimension of d_l in each layer $l \in \{1, ..., L\}$, binary mask $\boldsymbol{m_l} \in \{0,1\}^{d_l}$ yielding a sparse Neural Networks with sparse weights $\boldsymbol{\theta_l} \odot \boldsymbol{m_l}$. The sparsity level is the fraction of the weights that are zero-valued, calculated as $s = 1 - \frac{\sum_l \|\boldsymbol{m_l}\|_0}{\sum_l d_l}$.

Graph Neural Networks. GNNs denote a family of algorithms that extract structural information from graphs [35] and it is consisted of *Aggregate* and *Combine* operations. Usually, *Aggregate* is a function that aggregates messages from its neighbor nodes, and *Combine* is an update function that updates the representation of the current node. Formally, given the graph $\mathcal{G} = (\boldsymbol{A}, \boldsymbol{X})$ with node set $\mathcal{V}$ and edge set $\mathcal{E}$, the l-th layer of a GNN is represented as follows:

$$\boldsymbol{a}_v^l = Aggregate^l(\{\boldsymbol{h}_u^{l-1} : \forall u \in \mathcal{N}(v)\}) \tag{1}$$

$$\boldsymbol{h}_v^l = Combine^l(\boldsymbol{h}_v^{l-1}, \boldsymbol{a}_v^l) \tag{2}$$

where $\boldsymbol{a}_v^l$ is the aggregated representation of the neighborhood for node v and $\mathcal{N}(v)$ denotes the neighbor nodes set of the node v, and $\boldsymbol{h}_v^l$ is the node representations at the l-th layer. After propagating through L layers, we achieve the final node representations $\boldsymbol{h}_v^L$ which can be applied to downstream node-level tasks, such as node classification, link prediction.

Untrained Subnetworks. Following the prior work [11], [12] proposed Edge-Popup which enables finding untrained subnetworks hidden in the a randomly initialized full network $f(\boldsymbol{\theta})$ by solving the following discrete optimization problem:

$$\min_{\boldsymbol{m}(\boldsymbol{S}) \in \{0,1\}^{|\boldsymbol{\theta}|}} \mathcal{L}(f(\boldsymbol{X}; \boldsymbol{\theta} \odot \boldsymbol{m}(\boldsymbol{S})), \boldsymbol{y}) \tag{3}$$

where $\mathcal{L}$ is task-dependent loss function; $\odot$ represents an element-wise multiplication; $\boldsymbol{y}$ is the label for the input $\boldsymbol{X}$ and $\boldsymbol{m}$ is the binary mask that controls the sparsity level s. $\boldsymbol{S}$ is the latent score behind the binary mask $\boldsymbol{m}$ and it has the same dimension as $\boldsymbol{m}$. To avoid confusion, here we use $\boldsymbol{m}(\boldsymbol{S})$ instead of $\boldsymbol{m}$ to indicate that $\boldsymbol{m}$ is generated by $\boldsymbol{S}$. We will use $\boldsymbol{m}$ directly for brevity in the following content.

Different from the traditional training of deep neural networks, here the network weights are never updated, masks $\boldsymbol{m}$ are instead generated to search for the optimal untrained subnetwork. In practice, each mask $\boldsymbol{m}_i$ has a latent score variable $\boldsymbol{S}_i \in \mathcal{R}$ that represents the importance score of the corresponding weight $\boldsymbol{\theta}_i$. During training in the forward pass, the binary mask $\boldsymbol{m}$ is generated by setting top-s smallest elements of $\boldsymbol{S}$ to 0 otherwise 1. In the backward pass, all the values in $\boldsymbol{S}$ will be updated with straight-through estimation [36]. At the end of the training, an untrained subnetwork can be found by the generated mask $\boldsymbol{m}$ according to the converged scores $\boldsymbol{S}$.

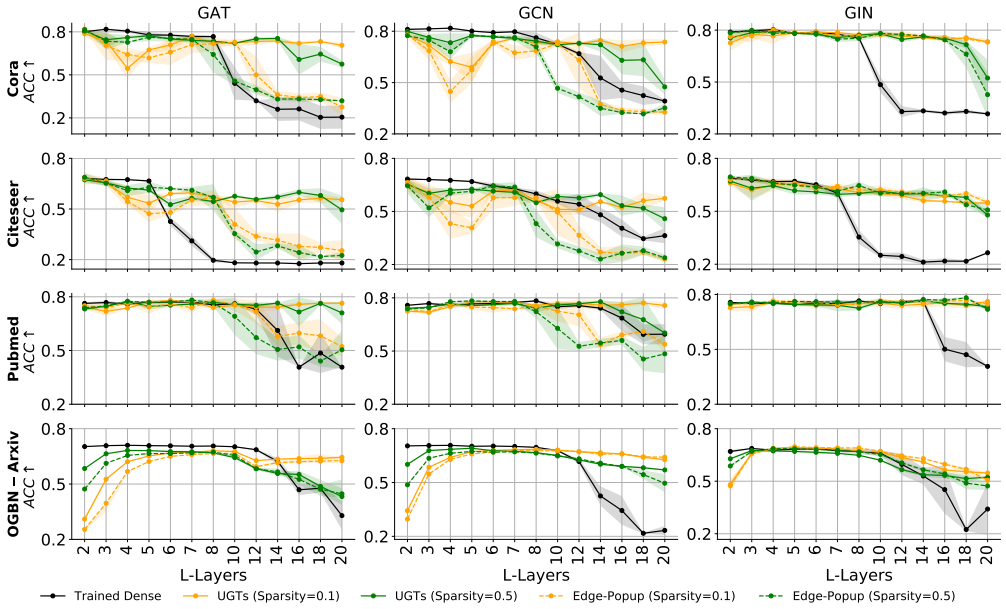

Figure 2: The performance of GNNs with increasing model depths. Experiments are conducted on various GNNs with Cora, Citeseer, Pubmed and OGBN-Arxiv. We observe that as the model goes deeper, fully-trained dense GNNs suffer from a sharp accuracy drop, while UGTs preserves the high accuracy. All the results reported are averaged from 5 runs.

3.2 Untrained GNNs Tickets – UGTs

In this section, we adopt the untrained subnetwork techniques to GNNs and introduce our new approach – Untrained GNNs Tickets (UGTs). We share the pseudocode of UGTs in the Appendix C.

Formally, given a graph neural network $g(\boldsymbol{A}, \boldsymbol{X}; \boldsymbol{\theta})$, where $\boldsymbol{A}$ and $\boldsymbol{X}$ are adjacency matrix and nodal features respectively. The optimization problem of finding an untrained subnetwork in GNNs can be therefore described as follows:

$$\min_{\boldsymbol{m} \in \{0,1\}^{|\boldsymbol{\theta}|}} \mathcal{L}(g(\boldsymbol{A}, \boldsymbol{X}; \boldsymbol{\theta} \odot \boldsymbol{m}), \boldsymbol{y}) \tag{4}$$

Although Edge-Popup [12] can find untrained subnetworks with proper predictive accuracy, its performance is still away from satisfactory. For instance, Edge-Popup can only obtain matching subnetworks at a relatively low sparsity i.e., 50%.

We highlight two limitations of the existing prior research. First of all, prior works [12, 13] **initially** set the sparsity level of $\boldsymbol{m}_i$ as s and maintain it throughout the optimization process. This is very appealing for the scenarios of sparse training [37–39] that chases a better trade-off between performance and efficiency, since the fixed sparsity usually translates to fewer floating-point operations (FLOPs). This scheme, however, is not necessary and perhaps harmful to the finding of the smallest possible untrained subnetwork that still performs well. Particularly as shown in [20], larger searching space for sparse neural networks at the early optimization phase leads to better sparse solutions. The second limitation is that the existing methods sparsify networks layer-wise with a uniform sparsity ratio, which typically leads to inferior performance compared with the non-uniform layer-wise sparsity [20, 39, 40], especially for deep architectures [41].

Untrained GNNs Tickets (UGTs). Leveraging the above-mentioned insights, we propose a new approach UGTs here which can discover matching untrained subnetworks with extremely high sparsity levels, i.e., up to 99%. Instead of keeping the sparsity of $\boldsymbol{m}$ fixed throughout the sparsification process, we start from an untrained dense GNNs and gradually increase the sparsity to the target sparsity during the whole sparsification process. We adjust the original gradual sparsification schedule [18, 19] to the linear decay schedule, since no big performance difference can be observed. The sparsity level s_t

Table 1: Test accuracy (%) of different training techniques. The experiments are based on GCN models with 16, 32 layers, respectively. Width is set to 448. See Appendix B.7 for GAT architecture. The results of the other methods are obtained from [42].

	Cora		Citeseer		Pubmed	
N-Layers	16	32	16	32	16	32
Trained Dense GCN	21.4	21.2	19.5	20.2	39.1	38.7
+Residual	20.1	19.6	20.8	20.90	38.8	38.7
+Jumping	76.0	75.5	58.3	55.0	75.6	75.3
+NodeNorm	21.5	21.4	18.8	19.1	18.9	18
+PairNorm	55.7	17.7	27.4	20.6	71.3	61.5
+DropNode	27.6	27.6	21.8	22.1	40.3	40.3
+DropEdge	28.0	27.8	22.9	22.9	40.6	40.5
UGTs-GCN	**77.3 ± 0.9**	**77.5 ± 0.8**	**61.1±0.9**	**56.2±0.4**	**77.6±0.9**	**76.3±1.2**

of each adjusting step t is calculated as follows:

$$s_t = s_f + (s_i - s_f)(1 - \frac{t - t_0}{n\Delta t}) \\ t \in \{t_0, t_0 + \Delta t, ..., t_0 + n\Delta t\} \tag{5}$$

where s_f and s_i refer to the final sparsity and initial sparsity, respectively; The initial sparsity is the sparsity at the start point of sparsification and it is set to 0 in this study. The final sparsity is the sparsity at the endpoint of sparsification. t_0 is the starting point of sparsification; Δt is the time between two adjusting steps; n is the total number of adjusting steps. We set Δt as one epoch of mask optimization in this paper.

To obtain a good non-uniform layer-wise sparsity ratio, we remove the weights with the smallest score values ($\boldsymbol{S}$) across layers at each adjusting step. We do this because [20] showed that the layer-wise sparsity obtained by this scheme outperforms the other well-studied sparsity ratios [19, 37, 39]. More importantly, removing weights across layers theoretically has a larger search space than solely considering one layer. The former can be more appealing as the GNN architecture goes deeper.

4 Experimental Results

In this section, we conduct extensive experiments among multiple GNN architectures and datasets to evaluate UGTs. We summarize the experimental setups here.

Table 2: Graph datasets statistics.

DataSets	#Graphs	#Nodes	#Edges	#Classes	#Features	Metric
Cora	1	2708	5429	7	1433	Accuracy
Citeseer	1	3327	4732	6	3703	Accuracy
Pubmed	1	19717	44338	3	3288	Accuracy
OGBN-Arxiv	1	169343	1166243	40	128	Accuracy
Texas	1	183	309	5	1703	Accuracy
OGBN-Products	1	24449029	61859140	47	100	Accuracy
OGBG-molhiv	41127	25.5(Average)	27.5(Average)	2	-	ROC-AUC
OGBG-molbace	1513	34.1(Average)	36.9(Average)	2	-	ROC-AUC

GNN Architectures. We use the three most widely used GNN architectures: GCN, GIN, and GAT [1] in our paper.

Datasets. We choose three popular small-scale graph datasets including Cora, Citeseer, PubMed [3] and one latest large-scale graph dataset OGBN-Arxiv [15] for our main experiments. To draw a solid conclusion, we also evaluate our method on other datasets including OGBN-Products [15], TEXAS [43], OGBG-molhiv [15] and OGBG-molbace [15, 44]. More detailed information can be found in Table 2.

[1] All experiments based on GAT architecture are conducted with heads=1 in this study.

4.1 The Existence of Matching Subnetworks

Figure 1 shows the effectiveness of UGTs with different GNNs, including GCN, GIN and GAT, on the four datasets. We can observe that as the model size increases, UGTs can find untrained subnetworks that match the fully-trained dense GNNs. This observation is perfectly in line with the previous findings [12, 13], which reveal that model size plays a crucial role to the existence of matching untrained subnetworks. Besides, it can be observed that the proposed UGTs consistently outperforms Edge-Popup across different settings.

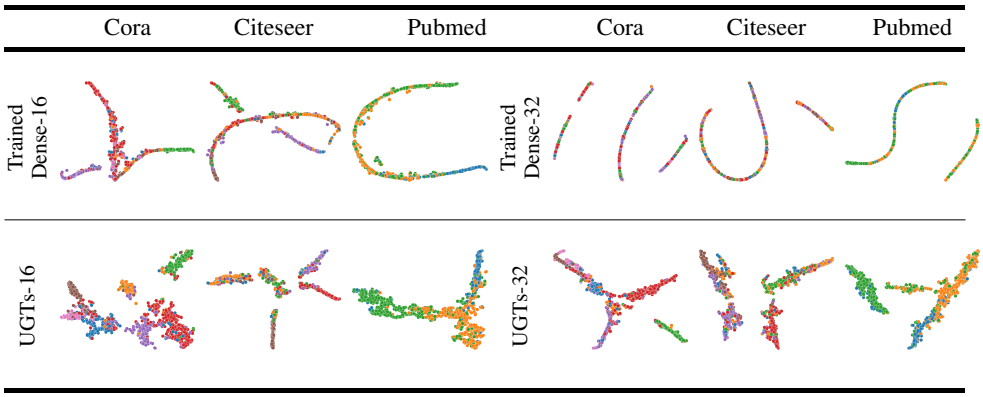

Figure 3: TSNE visualization of node representations learned by densely trained GCN and UGTs. Ten classes are randomly sampled from OGBN-Arxiv for visualization. Model depth is set as 16 and 32 respectively; width is set as 448. See Appendix B.1 for GAT architecture.

4.2 Over-smoothing Analysis

Deep architecture has been shown as a key factor that improves the model capability in computer vision [45]. However, it becomes less appealing in GNNs mainly because the node interaction through the message-passing mechanism (i.e., aggregation operator) would make node representations less distinguishable [26, 46], leading to a drastic drop of task performance. This phenomenon is well known as the over-smoothing problem [14, 42]. In this paper, we show a surprising result that UGTs can effectively mitigate over-smoothing in deep GNNs. We conduct extensive experiments to evaluate this claim in this section.

UGTs preserves the high accuracy as GNNs go deeper. In Figure 2, we vary the model depth of various architectures and report the test accuracy. All the experiments are conducted with architectures containing width 448 except for GAT on OGBN-Arxiv, in which we choose width 256 for GAT with $2 \sim 10$ layers and width 128 for GAT with $11 \sim 20$ layers, due to the memory limitation.

As we can see, the performance of trained dense GNNs suffers from a sharp performance drop when the model goes deeper, whereas UGTs impressively preserves the high accuracy across models. Especially at the mild sparsity, i.e., 0.1, UGTs almost has no deterioration with the increased number of layers.

UGTs achieves competitive performance with the well-versed training techniques. To further validate the effectiveness of UGTs in mitigating over-smoothing, we compare UGTs with six state-of-the-art techniques for the over-smoothing problem, including Residual connections, Jumping connections, NodeNorm, PairNorm, DropEdge, and DropNode. We follow the experimental setting in [42] and conduct experiments on Cora/Citeseer/Pubmed with GAT containing 16 and 32 layers. Model width is set to 448 for GAT on Cora/Citeseer/Pubmed. The results of the other methods are obtained from [42][2].

Table 1 shows that UGTs consistently outperforms all these advanced techniques on Cora, Citeseer, and Pubmed. For instance, UGTs outperforms the best performing technique (+Jumping) by 2.0%, 1.2%, 1.0% on Cora, Citeseer and Pubmed respectively with 32 layers. These results again verify our

[2] https://github.com/VITA-Group/Deep_GCN_Benchmarking.git

hypothesis that training bottlenecks of deep GNNs (e.g., over-smoothing) can be avoided or mitigated by finding untrained subnetworks without training weights at all.

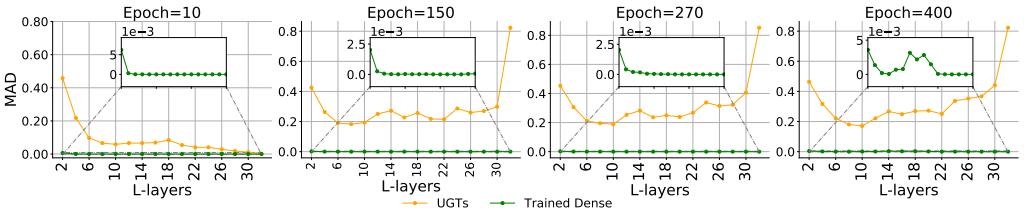

Figure 4: Mean Average Distance among node representations of each GNN layer. Experiments are conducted on Cora with GCN containing 32 layers and width 448.

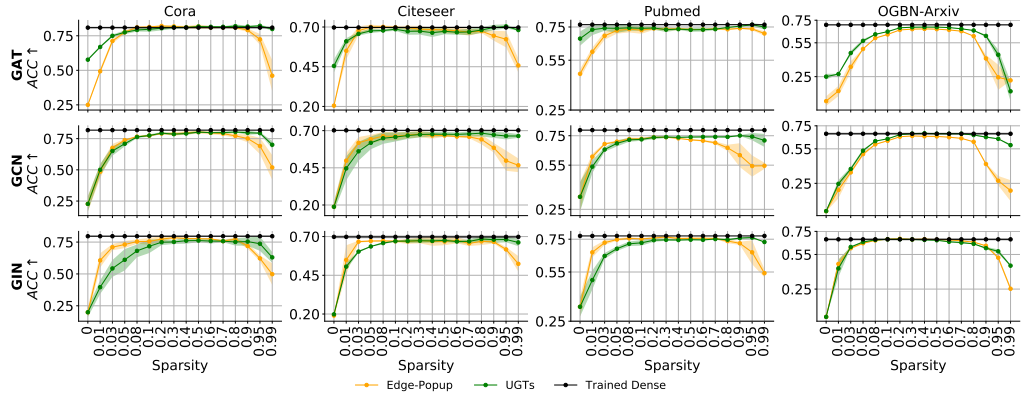

Figure 5: The accuracy of GNNs w.r.t varying sparsities. Experiments are conducted on various GNNs with 2 layers and width 256 for Cora, Citeseer and Pubmed, 4 layers and width 386 for OGBN-Arxiv.

Mean Average Distance (MAD). To further evaluate whether or not the good performance of UGTs can be contributed to the mitigation of over-smoothing, we visualize the smoothness of the node representations learned by UGTs and trained dense GNNs respectively. Following [46], we calculate the MAD distance among node representations for each layer during the process of sparsification. Concretely, MAD [46] is the quantitative metric for measuring the smoothness of the node representations. The smaller the MAD is, the smoother the node representations are. Results are reported in Figure 4. It can be observed that the node representations learned by UGTs keeps having a large distance throughout the optimization process, indicating a relieving of over-smoothing. On the contrary, the densely trained GCN suffers from severely indistinguishable representations of nodes.

TSNE Visualizations. Additionally, we visualize the node representations learned by UGTs and the trained dense GNNs with 16 and 32 layers, respectively, on both GCN and GAT architectures. Due to the limited space, we show the results of GCN in Figure 3 and put the visualization of GAT in the Appendix B.1. We can see that the node representations learned by the trained dense GCN are over-mixing in all scenarios and, in the deeper models (i.e., 32 layers), seem to be more indistinguishable. Meanwhile, the projection of node representations learned by UGTs maintains clearly distinguishable, again providing the empirical evidence of UGTs in mitigating over-smoothing problem.

4.3 The Effect of Sparsity on UGTs

To better understand the effect of sparsity on the performance of UGTs, we provide a comprehensive study in Figure 5 where the performance of UGTs with respect to different sparsity levels on different architectures. We summarize our observations below.

① UGTs consistently finds matching untrained graph subnetworks at a large range of sparsities, including the extreme ones. A matching untrained graph subnetwork can be identified with sparsities

from 0.1 even up to 0.99 on small-scale datasets such as Cora, Citeseer and Pubmed. For large-scale OGBN-Arxiv, it is more difficult to find matching untrained subnetworks. Matching subnetworks are mainly located within sparsities of $0.3 \sim 0.6$.

② **What's more, UGTs consistently outperforms Edge-Popup.** UGTs shows better performance than Edge-Popup at high sparsities across different architectures on Cora, Citeseer, Pubmed and OGBN-Arxiv. Surprisingly, increasing sparsity from 0.7 to 0.99, UGTs maintains very a high accuracy, whereas the accuracy of Edge-Popup shows a notable degradation. It is in accord with our expectation since UGTs finds important weights globally by searching for the well-performing sparse topology across layers.

4.4 Broader Evaluation of UGTs

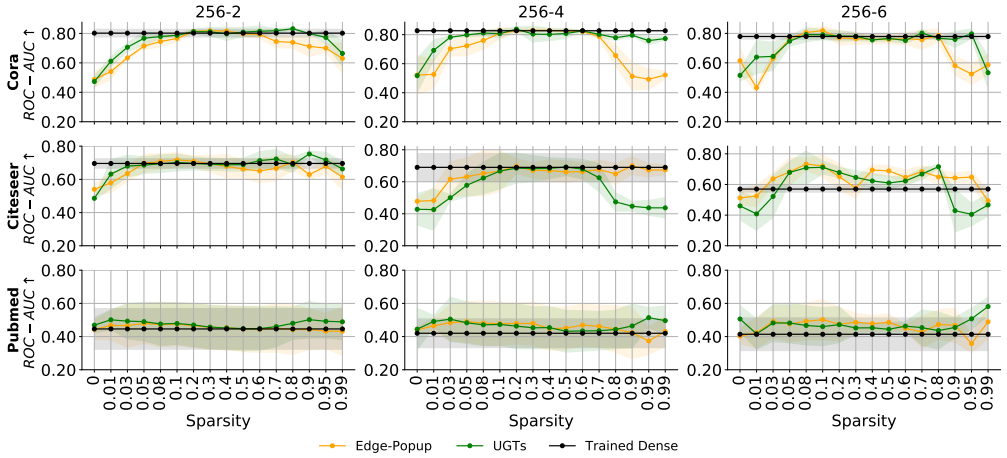

Figure 6: Out-of-distribution performance (ROC-AUC). Experiments are conducted with GCN (Width: 256, Depth: 2).

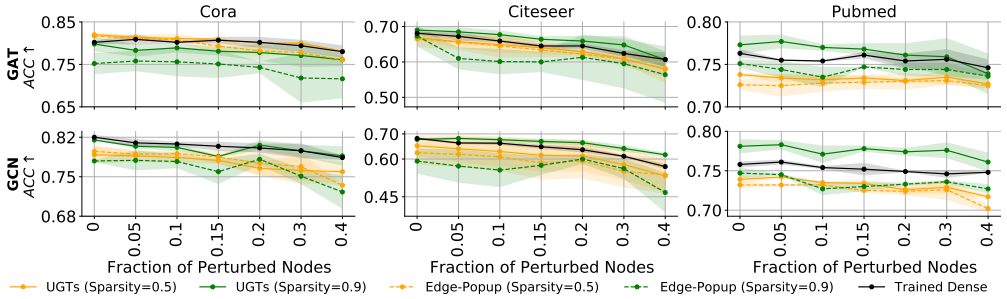

Figure 7: The robust performance on feature perturbations with the fraction of perturbed nodes varying from 0% to 40%. Experiments are conducted with GCN and GAT (Width: 256, Depth: 2).

In this section, we systematically study the performance of UGTs on out of distribution (OOD) detection, robustness against the input perturbations including feature and edge perturbations. Following [47], we create OOD samples by specifying all samples from 40% of classes and removing them from the training set. We create feature perturbations by replacing them with the noise sampled from Bernoulli distribution with p=0.5 and edge perturbations by moving edge's end point at random. The results of OOD experiments are reported in Figure 6 and Figure 10 (shown in Appendix B.2). The results of robustness experiments are reported in Figure 8 and Figure 7. We summarize our observations as follows:

① **UGTs enjoys matching performance on OOD detection.** Figure 6 and Figure 10 show that untrained graph subnetworks discovered by UGTs achieve matching performance on OOD detection compared with the trained dense GNNs in most cases. Besides, UGTs consistently outperforms Edge-Popup method at a large range of sparsities on OOD detection.

② **UGTs produces highly sparse yet robust subnetworks on input perturbations.** Figure 7 and Figure 8 demonstrate that UGTs with high sparsity level (Sparsity=0.9) achieves more robust results than the trained dense GNNs on both feature and edge perturbations with perturbation percentage ranging from 0 to 40%. Again, UGTs consistently outperforms Edge-Popup with both perturbation types.

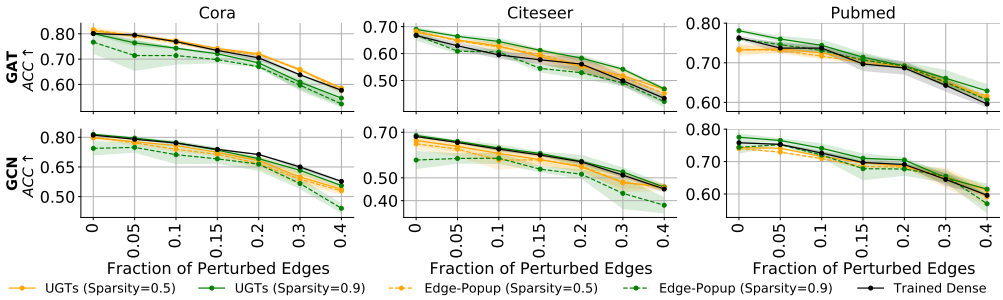

Figure 8: The robust performance on edge perturbations with the fraction of perturbed edges varying from 0% to 40%. Experiments are conducted with GCN and GAT (Width: 256, Depth: 2).

4.5 Experiments on Graph-level Task and Other Datasets

To draw a solid conclusion, we further conduct extensive experiments of graph-level task on OGBG-molhiv and OGBG-molbace; node-level task on TEXAS and OGBN-Products. The experiments are based on GCN model with width=448 and depth=3. Table 3 consistently verifies that a matching untrained subnetwork can be identified in GNNs across multiple tasks and datasets.

Table 3: Experments on graph-level tasks and other datasets. GCN Model with width:448, depth:3 are adopted for this experiments.

Node-level: OGBN-Products (Accuracy:%)											
Sparsity=	0.1	0.2	0.3	0.4	0.5	0.6	0.7	0.8	0.9	0.95	0.99
Dense	79.5	79.5	79.5	79.5	79.5	79.5	79.5	79.5	79.5	79.5	79.5
UGTs	75.6	77.7	78.7	77.8	79.3	79.5	79.9	78.6	74.5	64.1	35.3
Node-level: TEXAS (Accuracy:%)											
Dense	62.2	62.2	62.2	62.2	62.2	62.2	62.2	62.2	62.2	62.2	62.2
UGTs	62.1	62.2	62.2	62.2	62.2	61.3	62.2	63.1	64.8	64.8	55.8
Graph-level: OGBG-molhiv (ROCAUC:%)											
Dense	77.4	77.4	77.4	77.4	77.4	77.4	77.4	77.4	77.4	77.4	77.4
UGTs	76.4	76.9	76.5	76.1	76.3	77.3	75.8	77.1	73.1	75.3	75.1
Graph-level: OGBG-molbace (ROCAUC:%)											
Dense	78.3	78.3	78.3	78.3	78.3	78.3	78.3	78.3	78.3	78.3	78.3
UGTs	76.0	73.7	77.0	77.1	77.0	77.6	78.4	77.3	76.2	75.6	74.9

5 Conclusion

In this work, we for the first time confirm the existence of matching untrained subnetworks at a large range of sparsity. UGTs consistently outperforms the previous untrained technique – Edge-Popup on multiple graph datasets across various GNN architectures. What's more, we show a surprising result that searching for an untrained subnetwork within a randomly weighted dense GNN instead of directly training the latter can significantly mitigate the over-smoothing problem of deep GNNs. Across popular datasets, e.g., Cora, Citeseer, Pubmed, and OGBN-Arxiv, our method UGTs can achieve comparable or better performance with the various well-studied techniques that are specifically designed for over-smoothing. Moreover, we empirically find that UGTs also achieves appealing performance on other desirable aspects, such as out-of-distribution detection and robustness. The strong results of our paper point out a surprising but perhaps worth-a-try direction to obtain high-performing GNNs, i.e., finding the Untrained Tickets located within a randomly weighted dense GNN instead of training it.

References

[1] Franco Scarselli, Marco Gori, Ah Chung Tsoi, Markus Hagenbuchner, and Gabriele Monfardini. The graph neural network model. *IEEE transactions on neural networks*, 20(1):61–80, 2008. 1, 2

[2] Yujia Li, Daniel Tarlow, Marc Brockschmidt, and Richard Zemel. Gated graph sequence neural networks. In *International Conference on Learning Representations*, 2016. 1

[3] Thomas N Kipf and Max Welling. Semi-supervised classification with graph convolutional networks. *International Conference on Learning Representations*, 2017. 1, 2, 5, 13

[4] Keyulu Xu, Weihua Hu, Jure Leskovec, and Stefanie Jegelka. How powerful are graph neural networks? In *International Conference on Learning Representations*, 2019. URL `https://openreview.net/forum?id=ryGs6iA5Km`. 1, 2

[5] Petar Veličković, Guillem Cucurull, Arantxa Casanova, Adriana Romero, Pietro Lio, and Yoshua Bengio. Graph attention networks. *arXiv preprint arXiv:1710.10903*, 2017. 1, 2

[6] Jiezhong Qiu, Jian Tang, Hao Ma, Yuxiao Dong, Kuansan Wang, and Jie Tang. Deepinf: Social influence prediction with deep learning. In *Proceedings of the 24th ACM SIGKDD International Conference on Knowledge Discovery & Data Mining*, pages 2110–2119, 2018. 1

[7] Jia Li, Zhichao Han, Hong Cheng, Jiao Su, Pengyun Wang, Jianfeng Zhang, and Lujia Pan. Predicting path failure in time-evolving graphs. In *Proceedings of the 25th ACM SIGKDD International Conference on Knowledge Discovery & Data Mining*, pages 1279–1289, 2019. 1

[8] Marinka Zitnik and Jure Leskovec. Predicting multicellular function through multi-layer tissue networks. *Bioinformatics*, 33(14):i190–i198, 2017. 1, 2

[9] Shengnan Guo, Youfang Lin, Ning Feng, Chao Song, and Huaiyu Wan. Attention based spatial-temporal graph convolutional networks for traffic flow forecasting. In *Proceedings of the AAAI Conference on Artificial Intelligence*, volume 33, pages 922–929, 2019. 1

[10] Rex Ying, Ruining He, Kaifeng Chen, Pong Eksombatchai, William L Hamilton, and Jure Leskovec. Graph convolutional neural networks for web-scale recommender systems. In *Proceedings of the 24th ACM SIGKDD International Conference on Knowledge Discovery & Data Mining*, pages 974–983, 2018. 1

[11] Hattie Zhou, Janice Lan, Rosanne Liu, and Jason Yosinski. Deconstructing lottery tickets: Zeros, signs, and the supermask. *arXiv preprint arXiv:1905.01067*, 2019. 1, 2, 3

[12] Vivek Ramanujan, Mitchell Wortsman, Aniruddha Kembhavi, Ali Farhadi, and Mohammad Rastegari. What's hidden in a randomly weighted neural network? In *Proceedings of the IEEE/CVF Conference on Computer Vision and Pattern Recognition*, pages 11893–11902, 2020. 1, 2, 3, 4, 6

[13] Daiki Chijiwa, Shin'ya Yamaguchi, Yasutoshi Ida, Kenji Umakoshi, and Tomohiro Inoue. Pruning randomly initialized neural networks with iterative randomization. *arXiv preprint arXiv:2106.09269*, 2021. 1, 3, 4, 6

[14] Qimai Li, Zhichao Han, and Xiao-Ming Wu. Deeper insights into graph convolutional networks for semi-supervised learning. In *Thirty-Second AAAI conference on artificial intelligence*, 2018. 2, 6

[15] Weihua Hu, Matthias Fey, Marinka Zitnik, Yuxiao Dong, Hongyu Ren, Bowen Liu, Michele Catasta, and Jure Leskovec. Open graph benchmark: Datasets for machine learning on graphs. *arXiv preprint arXiv:2005.00687*, 2020. 2, 5, 13

[16] Jonathan Frankle and Michael Carbin. The lottery ticket hypothesis: Finding sparse, trainable neural networks. *arXiv preprint arXiv:1803.03635*, 2018. 2

[17] Tianlong Chen, Yongduo Sui, Xuxi Chen, Aston Zhang, and Zhangyang Wang. A unified lottery ticket hypothesis for graph neural networks. In *International Conference on Machine Learning*, pages 1695–1706. PMLR, 2021. 2

[18] Michael Zhu and Suyog Gupta. To prune, or not to prune: exploring the efficacy of pruning for model compression. *arXiv preprint arXiv:1710.01878*, 2017. 2, 4

[19] Trevor Gale, Erich Elsen, and Sara Hooker. The state of sparsity in deep neural networks. *arXiv preprint arXiv:1902.09574*, 2019. 2, 4, 5

[20] Shiwei Liu, Tianlong Chen, Xiaohan Chen, Zahra Atashgahi, Lu Yin, Huanyu Kou, Li Shen, Mykola Pechenizkiy, Zhangyang Wang, and Decebal Constantin Mocanu. Sparse training via boosting pruning plasticity with neuroregeneration. *Advances in Neural Information Processing Systems.*, 2021. 2, 4, 5

[21] William L Hamilton, Rex Ying, and Jure Leskovec. Inductive representation learning on large graphs. In *Proceedings of the 31st International Conference on Neural Information Processing Systems*, pages 1025–1035, 2017. 2

[22] Felix Wu, Amauri Souza, Tianyi Zhang, Christopher Fifty, Tao Yu, and Kilian Weinberger. Simplifying graph convolutional networks. In *International conference on machine learning*, pages 6861–6871. PMLR, 2019. 2

[23] Thomas N Kipf and Max Welling. Variational graph auto-encoders. *arXiv preprint arXiv:1611.07308*, 2016. 2

[24] Guohao Li, Matthias Muller, Ali Thabet, and Bernard Ghanem. Deepgcns: Can gcns go as deep as cnns? In *Proceedings of the IEEE/CVF International Conference on Computer Vision*, pages 9267–9276, 2019. 2

[25] Shunwang Gong, Mehdi Bahri, Michael M Bronstein, and Stefanos Zafeiriou. Geometrically principled connections in graph neural networks. In *Proceedings of the IEEE/CVF Conference on Computer Vision and Pattern Recognition*, pages 11415–11424, 2020. 2

[26] Lingxiao Zhao and Leman Akoglu. Pairnorm: Tackling oversmoothing in gnns. *arXiv preprint arXiv:1909.12223*, 2019. 2, 6

[27] Keyulu Xu, Chengtao Li, Yonglong Tian, Tomohiro Sonobe, Ken-ichi Kawarabayashi, and Stefanie Jegelka. Representation learning on graphs with jumping knowledge networks. In *International Conference on Machine Learning*, pages 5453–5462. PMLR, 2018. 2

[28] Meng Liu, Hongyang Gao, and Shuiwang Ji. Towards deeper graph neural networks. In *Proceedings of the 26th ACM SIGKDD International Conference on Knowledge Discovery & Data Mining*, pages 338–348, 2020. 2

[29] Ming Chen, Zhewei Wei, Zengfeng Huang, Bolin Ding, and Yaliang Li. Simple and deep graph convolutional networks. In *International Conference on Machine Learning*, pages 1725–1735. PMLR, 2020. 2

[30] Kuangqi Zhou, Yanfei Dong, Kaixin Wang, Wee Sun Lee, Bryan Hooi, Huan Xu, and Jiashi Feng. Understanding and resolving performance degradation in graph convolutional networks. *arXiv preprint arXiv:2006.07107*, 2020. 2

[31] Wenbing Huang, Yu Rong, Tingyang Xu, Fuchun Sun, and Junzhou Huang. Tackling over-smoothing for general graph convolutional networks. *arXiv preprint arXiv:2008.09864*, 2020. 2

[32] Yu Rong, Wenbing Huang, Tingyang Xu, and Junzhou Huang. Dropedge: Towards deep graph convolutional networks on node classification. *arXiv preprint arXiv:1907.10903*, 2019. 2

[33] Mitchell Wortsman, Vivek Ramanujan, Rosanne Liu, Aniruddha Kembhavi, Mohammad Rastegari, Jason Yosinski, and Ali Farhadi. Supermasks in superposition. *arXiv preprint arXiv:2006.14769*, 2020. 3

[34] Yonggan Fu, Qixuan Yu, Yang Zhang, Shang Wu, Xu Ouyang, David Cox, and Yingyan Lin. Drawing robust scratch tickets: Subnetworks with inborn robustness are found within randomly initialized networks. *Advances in Neural Information Processing Systems*, 34, 2021. 3

[35] William L Hamilton, Rex Ying, and Jure Leskovec. Representation learning on graphs: Methods and applications. *arXiv preprint arXiv:1709.05584*, 2017. 3

[36] Yoshua Bengio, Nicholas Léonard, and Aaron Courville. Estimating or propagating gradients through stochastic neurons for conditional computation. *arXiv preprint arXiv:1308.3432*, 2013. 3

[37] Decebal Constantin Mocanu, Elena Mocanu, Peter Stone, Phuong H Nguyen, Madeleine Gibescu, and Antonio Liotta. Scalable training of artificial neural networks with adaptive sparse connectivity inspired by network science. *Nature communications*, 9(1):1–12, 2018. 4, 5

[38] Shiwei Liu, Decebal Constantin Mocanu, Amarsagar Reddy Ramapuram Matavalam, Yulong Pei, and Mykola Pechenizkiy. Sparse evolutionary deep learning with over one million artificial neurons on commodity hardware. *Neural Computing and Applications*, 2020.

[39] Utku Evci, Trevor Gale, Jacob Menick, Pablo Samuel Castro, and Erich Elsen. Rigging the lottery: Making all tickets winners. In *International Conference on Machine Learning*, pages 2943–2952. PMLR, 2020. 4, 5

[40] Aditya Kusupati, Vivek Ramanujan, Raghav Somani, Mitchell Wortsman, Prateek Jain, Sham Kakade, and Ali Farhadi. Soft threshold weight reparameterization for learnable sparsity. In *International Conference on Machine Learning*, 2020. 4

[41] Tim Dettmers and Luke Zettlemoyer. Sparse networks from scratch: Faster training without losing performance. *arXiv preprint arXiv:1907.04840*, 2019. 4

[42] Tianlong Chen, Kaixiong Zhou, Keyu Duan, Wenqing Zheng, Peihao Wang, Xia Hu, and Zhangyang Wang. Bag of tricks for training deeper graph neural networks: A comprehensive benchmark study. *arXiv preprint arXiv:2108.10521*, 2021. 5, 6, 13

[43] Hongbin Pei, Bingzhe Wei, Kevin Chen-Chuan Chang, Yu Lei, and Bo Yang. Geom-gcn: Geometric graph convolutional networks. *arXiv preprint arXiv:2002.05287*, 2020. 5

[44] Zhenqin Wu, Bharath Ramsundar, Evan N Feinberg, Joseph Gomes, Caleb Geniesse, Aneesh S Pappu, Karl Leswing, and Vijay Pande. Moleculenet: a benchmark for molecular machine learning. *Chemical science*, 9(2):513–530, 2018. 5

[45] Kaiming He, Xiangyu Zhang, Shaoqing Ren, and Jian Sun. Deep residual learning for image recognition. In *Proceedings of the IEEE conference on computer vision and pattern recognition*, pages 770–778, 2016. 6

[46] Deli Chen, Yankai Lin, Wei Li, Peng Li, Jie Zhou, and Xu Sun. Measuring and relieving the over-smoothing problem for graph neural networks from the topological view. In *Proceedings of the AAAI Conference on Artificial Intelligence*, volume 34, pages 3438–3445, 2020. 6, 7

[47] Maximilian Stadler, Bertrand Charpentier, Simon Geisler, Daniel Zügner, and Stephan Günnemann. Graph posterior network: Bayesian predictive uncertainty for node classification. *Advances in Neural Information Processing Systems*, 34, 2021. 8

[48] Chengxuan Ying, Tianle Cai, Shengjie Luo, Shuxin Zheng, Guolin Ke, Di He, Yanming Shen, and Tie-Yan Liu. Do transformers really perform bad for graph representation? *arXiv preprint arXiv:2106.05234*, 2021. 13

A Implementation Details

In this paper, all experiments on Cora/Citeseer/Pubmed datasets are conducted on 1 GeForce RTX 2080TI (11GB) and all experiments on OGBN-Arxiv are conducted on 1 DGX-A100 (40GB). All the results reported in this paper are conducted by 5 independent repeated runs.

Train-Val-Test splitting Datasets We use 140 (Cora), 120 (Citeseer) and 60 (PubMed) labeled data for training, 500 nodes for validation and 1000 nodes for testing. We follow the strategy in [15] for splitting OGBN-Arxiv dataset.

Hyper-parameter Configuration We follow [3, 42, 48] to configure the hyper-parameters for training dense GNN models. All hyper-parameters configurations for UGTs are summarized in Table 4.

Table 4: Implementation details for UGTs.

DataSets	Cora	Citeseer	Pubmed	OGBN-Arxiv
Total Epoches	400	400	400	400
Learning Rate	0.01	0.01	0.01	0.01 (GNNs with Layers<10) 0.001(GNNs with Layers>10)
Optimizer	Adam	Adam	Adam	Adam
Weight Decay	0.0	0.0	0.0	0.0
n(total adjustion epoches)	200	200	200	200
t_0	0	0	0	0
Δt	1 epoch	1 epoch	1 epoch	1 epoch

B More Experimental Results

B.1 TSNE visualization.

Figure 9 provides the TSNE visualization for node representations learned by UGTs and dense GAT. It can be observed that the node representations learned by the trained dense GAT are mixed while the node representations learned by UGTs are disentangled.

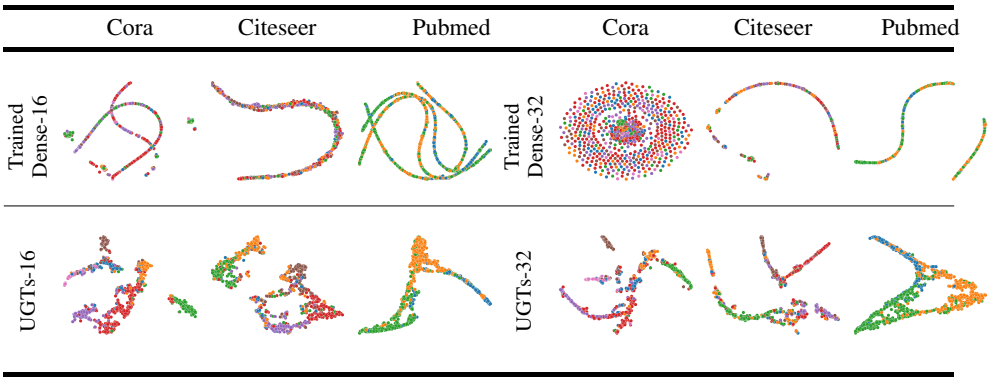

Figure 9: TSNE visualization for node representations. Experiments are based on GAT with fixed width 448.

B.2 Out of distribution detection

Figure 10 shows the OOD performance for UGTs and the trained dense GNNs based on GAT architecture. As we can observe, UGTs achieves very appealing results on OOD performance than the corresponding trained dense GAT.

B.3 Robustness against input perturbations

In this section, we explore the robustness against input perturbations with varying the sparsity of untrained GNNs. Experiments are conducted on GAT and GCN architectures with width=256 and depth=2. Results are reported in Figure 12 and Figure 11.

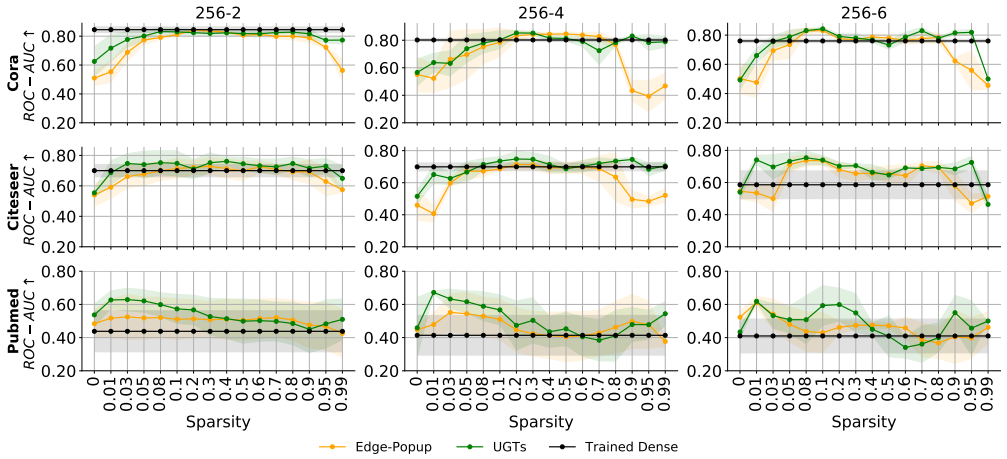

Figure 10: Out-of-distribution performance (ROC-AUC). Experiments are based on GAT architecture (Width:256, Depth:2)

It can be observed that the robustness achieved by UGTs is increasing with the increase of sparsity for both edge and feature perturbation types. Besides, the robustness achieved by UGTs at large sparsity, e.g., sparsity =0.9, can outperform the counterpart trained dense GNNs.

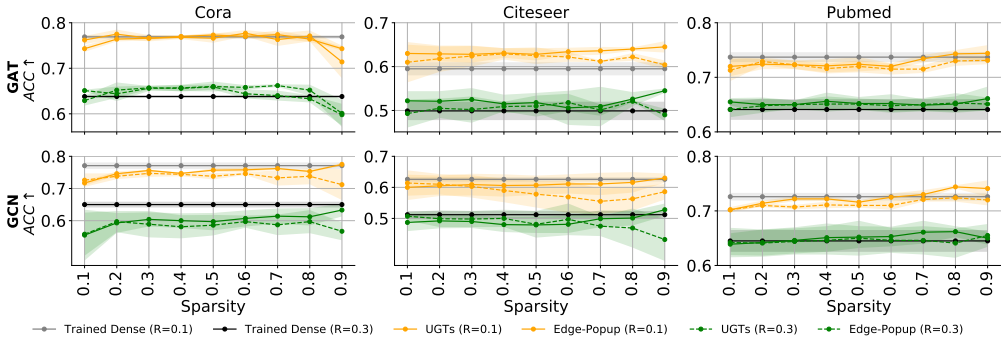

Figure 11: The robust performance on edge perturbations.R denotes the fraction of perturbed edges.(width:256, Depth:2)

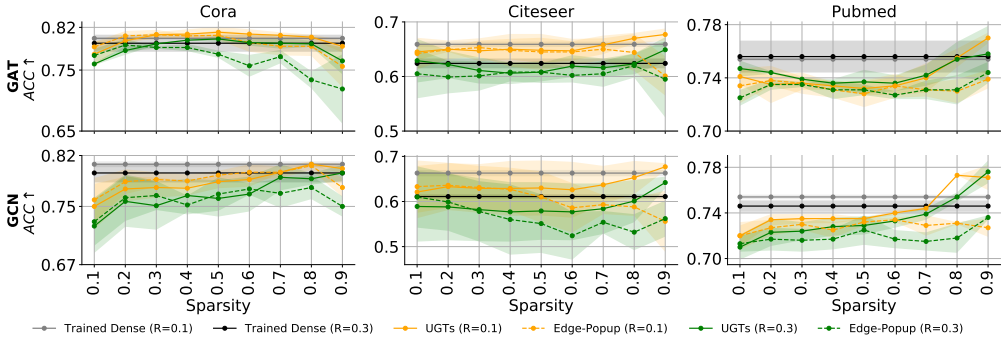

Figure 12: The robust performance on feature perturbations.R denotes the fraction of perturbed nodes. (width:256, Depth:2)

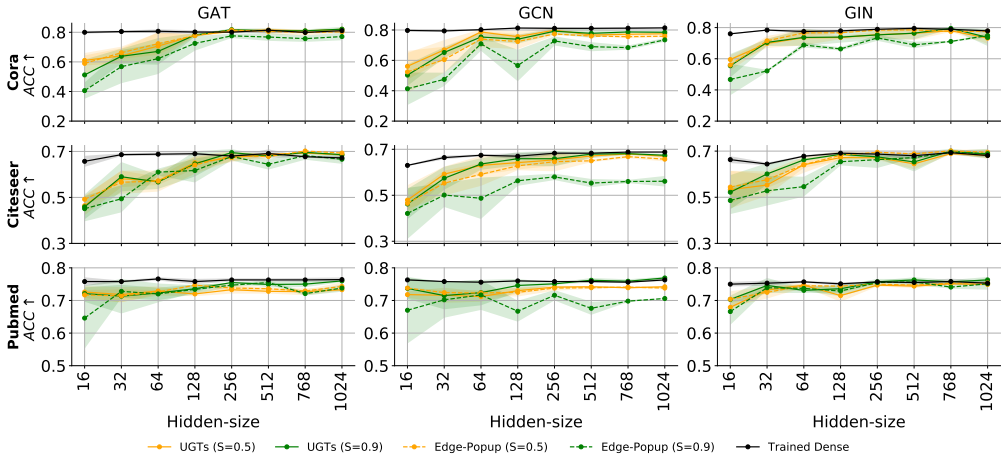

Figure 13: Model Width: The accuracy performance of subnetworks from untrained GNNs w.r.t varying Hidden-Size. The "S01,S05,S09" represents the sparsity of the untrained GNNs. The dashed line represents the results of the trained dense GNNs. Experiments are based on GNNs with 2 layers.

B.4 The accuracy performance w.r.t model width

Figure 13 shows the performance of UGTs on different architectures with varying model width from 16 to 1024 and fix depth=2. We summarize observations as follows:

① **Performance of UGTs improves with the width of the GNN models.** With width increasing from 16 to 256, the performance of UGTs improves apparently and after width=256, the benefits from model width are saturated.

B.5 Ablation studies

We conduct the ablation studies to show the effectiveness of UGTs.The results showed on Table 5. Compared with Edge-Popup, UGTs mainly has two novelties: global sparsification (VS. uniform sparsification) and gradual sparsification (VS. one-shot sparsification). Here we compare UGTs with 3 baselines: (1) UGTs - global sparsification; (2) UGTs - gradual sparsification; (3) Edge-Popup. The results are reported in the following table and it shows that global sparsification plays an important role for finding important weights and gradual sparsification is crucial for further boosting performance at high sparsity level.

Table 5: Ablation studies based on GAT (Depth:2, Width:256) and Cora.

	0.1	0.3	0.5	0.7	0.9	0.95
Edge-Popup	**0.814**	0.81	0.809	0.81	0.791	0.461
UGTs - global sparsification	0.807	0.816	0.817	0.804	0.799	0.731
UGTs - gradual sparsification	0.806	**0.818**	**0.821**	**0.821**	0.804	0.795
UGTs	0.797	0.811	0.81	0.815	**0.817**	**0.822**

B.6 Observations via gradient norm

To preliminary understand why UGTs can mitigate over-smoothing while the trained dense GNNs can not, we calculate the gradient norm of each layer for UGTs and dense GCN during training. In order to have a fair comparison, we calculate the gradient norm of $\nabla_{(\boldsymbol{m}^l \odot \boldsymbol{\theta}^l)} \mathcal{L}(g(\boldsymbol{A}, \boldsymbol{X}; \boldsymbol{\theta} \odot \boldsymbol{m}), y)$ for UGTs and the gradient norm of $\nabla_{\boldsymbol{\theta}^l} \mathcal{L}(g(\boldsymbol{A}, \boldsymbol{X}; \boldsymbol{\theta}), y)$ for dense GCN where l denotes the layer. Results are reported in Figure 14.

As we can observe, the gradient vanishing problem may exist for training deep dense GCN since the gradient norm for dense GCN is extremely small while UGTs does not have this problem. This problem might also be indicated by the training loss where the training loss for dense GCN does not

decrease while the training loss for UGTs decreases a lot. This might explain why UGTs performs well for deep GNNs.

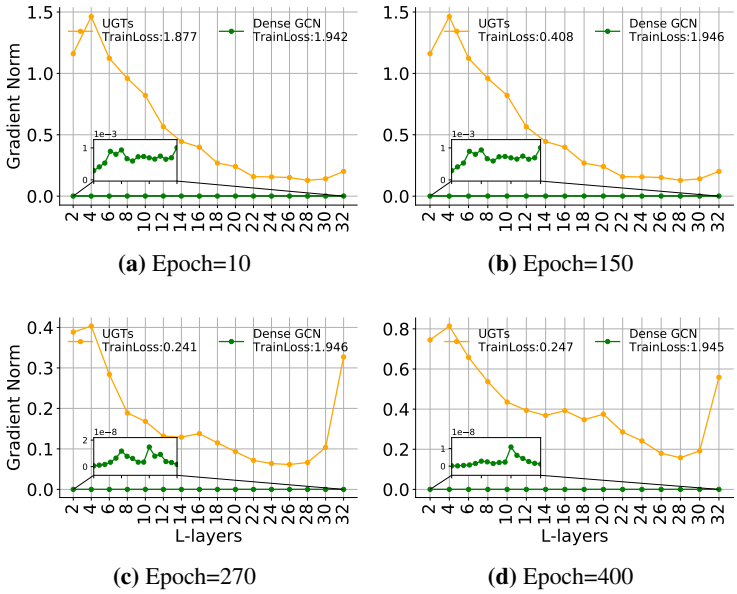

(a) Epoch=10 **(b)** Epoch=150

(c) Epoch=270 **(d)** Epoch=400

Figure 14: Gradient norm w.r.t each layer during training. Experiments are conducted on Cora with GCN architecture containing 32 layers and width 448.

B.7 More experiments for mitigating over-smoothing problem

We conduct experiments on Cora, Citeseer and Pubmed for GAT with deeper layers. The width is fixed to 448. The results of the other methods are obtained by running the code[3].

The results are reported in Table 6. It can be observed again that UGTs consistently outperforms all the baselines.

Table 6: Test accuracy (%) of different training techniques. The experiments are based on GAT models with 16, 32 layers, respectively. Width is set to 448.

	Cora		Citeseer		Pubmed	
N-Layers	16	32	16	32	16	32
Trained Dense GAT	20.6	13.0	20.0	16.9	17.9	18.0
+Residual	19.9	20.7	17.7	19.2	41.6	40.8
+Jumping	39.7	27.8	29.1	25.5	57.3	57.1
+NodeNorm	70.9	11.0	17.1	18.4	72.2	59.7
+PairNorm	27.9	12.1	22.8	17.7	73.0	44.0
+DropNode	23.6	13.0	18.8	7.0	26.7	18.0
+DropEdge	24.8	13.0	19.4	7.0	19.3	18.0
UGTs-GAT	**76.7 ± 1.1**	**74.9±0.2**	**62.7±0.7**	**56.5±1.1**	**77.9±0.5**	**75.5±1.5**

C Pseudocode

Pseudocode is showed in Algothrim 1.

[3] https://github.com/VITA-Group/Deep_GCN_Benchmarking.git

Algorithm 1 Untrained GNNs Tickets (UGTs)

Input: a GNN $g(\boldsymbol{A}, \boldsymbol{X}; \boldsymbol{\theta})$, initial mask $\boldsymbol{m} = 1 \in \mathcal{R}^{|\boldsymbol{\theta}|}$ with latent scores $\boldsymbol{S}$, learning rate λ, hyperparameters for the gradual sparsification schedule s_i, s_f, t_0, and Δt.
Output: $g(\boldsymbol{A}, \boldsymbol{X}; \boldsymbol{\theta} \odot \boldsymbol{m}), \boldsymbol{y}$
Randomly initialize model weights $\boldsymbol{\theta}$ and $\boldsymbol{S}$.
for $t = 1$ **to** T **do**
  #Calculate the current sparsity level s_t by Eq. 5.
  $s_t \longleftarrow s_f + (s_i - s_f)(1 - \frac{t - t_0}{n \Delta t})$
  #Get the global threshold value at top s_t by sorting $\boldsymbol{S}$ in ascending order.
  $\boldsymbol{S}_{thres} \longleftarrow Thresholding(\boldsymbol{S}, s_t)$
  #Generate the binary mask.
  $\boldsymbol{m} \longleftarrow 0$ if $\boldsymbol{S} < \boldsymbol{S}_{thres}$ else 1
  #Update $\boldsymbol{S}$.
  $\boldsymbol{S} \longleftarrow \boldsymbol{S} - \lambda \nabla_{\boldsymbol{S}} \mathcal{L}(g(A, \boldsymbol{X}; \boldsymbol{\theta} \odot \boldsymbol{m}), \boldsymbol{y})$
end for
Return $g(\boldsymbol{A}, \boldsymbol{X}; \boldsymbol{\theta} \odot \boldsymbol{m}), \boldsymbol{y}$